International Journal of Biological Macromolecules 267 (2024) 131581

Contents lists available at ScienceDirect

International Journal of Biological Macromolecules

journal homepage: www.elsevier.com/locate/ijbiomac

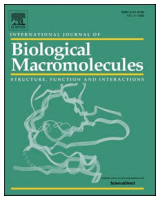

Modulation of bacterial membranes and cellular macromolecules by dimethyl sulfoxide: A dose-dependent study providing novel insights

Sinem Tunçer Çağlayan [a,*], Rafig Gurbanov [b,c]

[a] Vocational School of Health Services, Department of Medical Services and Techniques, Bilecik Şeyh Edebali University, 11100 Bilecik, Turkey
[b] Department of Bioengineering, Bilecik Şeyh Edebali University, 11100 Bilecik, Turkey
[c] Central Research Laboratory, Bilecik Şeyh Edebali University, 11100 Bilecik, Turkey

ARTICLE INFO

Keywords:
Dimethyl sulfoxide
Bacteria
Membrane potential
Zeta potential
Fourier-transform infrared (FT-IR) spectroscopy

ABSTRACT

Using *Escherichia coli* as a model, this manuscript delves into the intricate interactions between dimethyl sulfoxide (DMSO) and membranes, cellular macromolecules, and the effects on various aspects of bacterial physiology. Given DMSO's wide-ranging use as a solvent in microbiology, we investigate the impacts of both non-growth inhibitory (1.0 % and 2.5 % *v*/v) and slightly growth-inhibitory (5.0 % v/v) concentrations of DMSO. The results demonstrate that DMSO causes alterations in bacterial membrane potential, influences the electrochemical characteristics of the cell surface, and exerts substantial effects on the composition and structure of cellular biomolecules. Genome-wide gene expression data from DMSO-treated *E. coli* was used to further investigate and bolster the results. The findings of this study provide valuable insights into the complex relationship between DMSO and biological systems, with potential implications in drug delivery and cellular manipulation. However, it is essential to exercise caution when utilizing DMSO to enhance the solubility and delivery of bioactive compounds, as even at low concentrations, DMSO exerts non-inert effects on cellular macromolecules and processes.

1. Introduction

Dimethyl sulfoxide (DMSO; C_2H_6OS) was initially synthesized by the Russian organic chemist Alexander Zaytsev through the oxidation of dimethyl sulfide, a byproduct of the kraft process [1]. DMSO is a small molecule characterized by a hydrophilic sulfoxide group and two hydrophobic methyl groups, rendering it capable of solubilizing both polar and non-polar substances and overcoming hydrophobic barriers [2]. In addition to its solvent properties, DMSO exhibits various biological and medical activities which were well documented by Jacob and De La Torre [1]. For instance, DMSO has been recognized as an inducer of mammalian cell differentiation [3,4], hydrogen bond disruptor, hydroxyl radical scavenger, intracellular low-density lipoprotein-derived cholesterol mobilizer, molecular (or chemical) chaperone [1,5], and cell membrane fusing agent [6]. Moreover, DMSO is widely employed in cryopreservation, particularly in cell culture laboratories, where it protects the cells against mechanical damage induced by ice crystal formation [7]. Furthermore, DMSO is utilized in various pharmaceutical products, either as an active ingredient or an excipient [8], and is a common component in numerous approved topical pharmaceutical formulations, known for its ability to facilitate penetration [9].

Solubility is a critical parameter in evaluating a compound's biological effects and ascertaining its cellular and systemic bioavailability. DMSO's amphipathic properties make it exceptionally well-suited for dissolving both poorly soluble polar and non-polar test compounds [10]. Therefore, DMSO is frequently endorsed as a solvent for a variety of applications, encompassing established methods for screening the antimicrobial properties of synthetic and natural molecules. Moreover, it has seen extensive use over the years in the fields of toxicology and experimental pharmacology [11]. DMSO is widely acknowledged as safe, which often leads to the omission of reported solvent concentrations in most publications, assuming that its effects are negligible [10]. However, when eukaryotic cells were employed as models, we, along with other researchers, observed that DMSO induces various changes in cellular macromolecules, even at very low concentrations that do not affect cell viability [7,12,13]. In addition, our recent study using *E. coli* (ATCC 8739) as a model has unveiled that non-toxic DMSO concentrations (1.0 and 2.5 %, *v*/v) influence cellular nucleic acid content, modify DNA topology, alter the global 5-methylcytosine (5-mC) pattern of the genome, and modulate gene transcription. These findings indicate that

* Corresponding author.
E-mail address: sinem.tuncer@bilecik.edu.tr (S. Tunçer Çağlayan).

https://doi.org/10.1016/j.ijbiomac.2024.131581
Received 10 November 2023; Received in revised form 10 April 2024; Accepted 11 April 2024
Available online 12 April 2024

even at low concentrations, DMSO exerts non-inert effects on bacterial cells [14].

It is extensively documented that DMSO enhances membrane permeability in eukaryotes, thus facilitating the delivery of drugs across biological membranes. Additionally, the cryoprotective attributes of DMSO are linked to its capacity to modulate membrane permeability [15]. Simulations involving model membranes and studies conducted on mammalian cells have illustrated that DMSO can modify the structure and characteristics of cell membranes, even at low concentrations (0.1–2 %, *v*/v) [16]. Previously we showed that 1.0 % and 2.5 % DMSO do not affect the cellular viability of the *E. coli* strain Crooks (ATCC 8739), a routinely used reference strain in testing antimicrobial formulations [17]; however, 5.0 % DMSO caused a slight (3.5 %) but significant change ($p = 0.0078$) in the growth of the bacteria [14]. Here, we investigated the effects of low-dose, non-toxic (1.0 and 2.5 %, *v*/v) DMSO treatment in comparison with the effects of a moderate growth-inhibitory concentration of DMSO (5.0 %, v/v) on bacterial membranes and cellular macromolecules. To the best of our knowledge, for the first time in the literature, we demonstrate that DMSO treatment induces dose-dependent changes in the bacterial membrane potential, as well as modulates the electrochemical properties of the cell surface, in addition to its considerable effects on the content and structure of cellular biomolecules. *In silico* analysis of the transcriptome data from the DMSO-treated bacteria shows that some of these effects can be attributed to DMSO-induced changes in gene expression.

2. Materials and methods

2.1. Bacterial culture and DMSO treatment

E. coli strain Crooks (ATCC 8739) was grown aerobically in Nutrient broth (Nutrient Broth for Microbiology, No. 1, Fluka, Germany) and treated with DMSO as described before [14]. Briefly, following overnight culturing at 37 °C in a 160 rpm shaking incubator, the optical density of the overnight culture was diluted to OD_{600} of 0.1 before the treatments (1.0 %, 2.5 %, or 5.0 %, *v*/v) with sterile, cell culture grade DMSO (Santa Cruz Biotechnology, Germany). Control groups (Untreated-UT) were left untreated. To determine the growth dynamics of the DMSO-treated cultures, the optical densities of the cultures at 600 nm were measured every 2 h for 24 h. The growth curve, which was presented before in our previous study [14], indicated that the culture transitioned into the stationary phase following 10 h of incubation. It has been reported that changes in morphology and physiology become apparent as bacteria enter the stationary phase, coinciding with the development of heightened resistance to various stresses [18]. Besides, *E. coli* exposed to stresses would respond to counteract the effects and it is able to adapt to the culture additives [19]. Consequently, all experiments were conducted on bacteria during the late logarithmic (to early stationary phase), specifically after 10 h of incubation as described before [14,20,21].

2.2. Measurement of membrane potential

The BacLight™ Bacterial Membrane Potential Kit (Invitrogen, Waltham, Massachusetts, USA) was employed according to the manufacturer's instructions. The impact of DMSO treatment on membrane potential was evaluated after a 10 h incubation, during the late log-phase cultures, as recommended in the instructions. Briefly, 1×10^6 cells (both DMSO-treated and untreated bacteria) were diluted in 1 mL of 0.22 μm pore size membrane-filtered 1× Phosphate Buffered Saline (PBS). For the depolarized control sample, 10 μL of 500 μM CCCP (carbonyl cyanide 3-chlorophenylhydrazone, Component B) was added to the untreated sample. In each case, except for the unstained control, 10 μL of 3 mM fluorescent membrane-potential indicator dye $DiOC_2$ (3,3′-diethyloxacarbocyanine iodide, Component A) was added, mixed, and the samples were incubated at RT for 15 min. Following incubation, the samples were analyzed using the BD Accuri flow cytometer (BD Biosciences, Franklin Lakes, New Jersey, USA) with FL1 (green fluorescence) and FL3 (red fluorescence) detectors. 10000 events were examined for each measurement and forward scatter (FSC) and side scatter (SSC) dot plots were used to determine the cell populations.

$DiOC_2$ emits green fluorescence within bacterial cells. However, an elevated membrane potential leads to an increase in the cytoplasmic concentration of the dye, causing the dye molecules to aggregate and resulting in a shift toward red fluorescence emission. CCCP, acting as a proton ionophore, reduces membrane potential, thereby preventing the detection of red fluorescence. In the experiments, CCCP treatment served as the control, and the FL1 and FL3 signals from cells incubated with CCCP were used to create a dot plot for gating. Consequently, for each sample, changes in membrane potential were calculated as the ratio of FL3% to FL1%. The results, based on two independent experiments, each with three technical replicates, were presented as fold changes relative to the untreated control.

2.3. Zeta potential measurements

To determine the effect of DMSO on zeta potential, at the end of the incubation period, the cultures were diluted to $OD_{600} = 0.3$ in 1 mL of dH_2O (passed through a 0.22 μm filter). Following dilution, centrifugation was performed at 3300 ×*g* for 5 min at RT. The pellet was suspended in 1 mL of dH_2O (refraction index: 1.333), and Zeta potential measurements were conducted for each sample using Zetasizer-NANO-ZS (Malvern Instruments, UK) [22]. The experiments were performed with two biological replicates, and each replicate was sampled three times.

2.4. In silico analysis

The publically available RNA sequencing data was analyzed as described before [14] by quantifying the differentially expressed genes ($p > 0.9$) using an edgeR R package (http://bioconductor.org/packages/release/bioc/html/edgeR.html). Gene Ontology (GO) and Kyoto Encyclopedia of Genes and Genomes (KEGG) pathway analyses were performed using the "Functional Annotation" module in the OmicsBox tool (https://www.biobam.com/omicsbox/). The data is accessible at the Sequence Read Archive (SRA) hosted by NCBI (https://www.ncbi.nlm.nih.gov/), under the bioproject PRJNA777047. The corresponding SRA accession numbers for the untreated control sample, along with the 1.0 % and 2.5 % DMSO-treated samples, are as follows: SRR16690734, SRR16690860, and SRR16691093.

2.5. Infrared spectroscopy and chemometric analyses

ATR-FTIR spectroscopy was applied as described before [14]. Concisely, after two times washing by centrifugation in a benchtop centrifuge at RT (5000xrpm, 10 min) in PBS, the cells were suspended as 10^7 cells/μL in PBS and 5 μL of suspension was placed on the Zn/Se crystal of the ATR unit (PerkinElmer, Waltham, Massachusetts, USA). The samples were examined at a resolution of 2 cm^{-1} and a scan number 32. The spectra were obtained with the Spectrum One (PerkinElmer) software in the wavelength range of 4000–650 cm^{-1}. PBS, which was used to suspend the cells, was scanned under identical experimental conditions as the samples and manually subtracted from the sample spectra. The free water band located around 2125 cm^{-1} was flattened to eliminate the effect of PBS during the process of subtraction. The difference spectra were used for all further spectral analyses performed using OPUS 5.5 (Bruker, Billerica, Massachusetts, USA) software. The second-derivative spectra of each sample were obtained and vector-normalized using 9 smoothing points. Subsequently, the absolute intensities of spectral sub-bands were quantified using the standard Peak Picking Method (peak directions: minima) in OPUS 5.5 (Bruker) software.

Principal Component Analysis (PCA) and Hierarchical Cluster Analysis (HCA) are widely used unsupervised chemometric methods. PCA transforms a set of related variables into a smaller group of distinct variables known as principal components (PCs). A condensed PC model can quickly identify and distinguish deviations within the initial system. The higher-order PCs, such as PC1, elucidate the most significant sources of variance in the dataset and generally account for the prominent spectral changes. This approach is precious when conducting a robust analysis of the comprehensive dataset [7]. Here, PCA was applied to ATR-FTIR infrared (IR) spectral data to perform an exploratory analysis of the experimental groups as previously described [23,24]. Briefly, each group's unit vector-normalized and mean-centered spectra were imported into The Unscrambler® X 10.3 (CAMO Software AS, Norway) multivariate analysis (MVA) software. PCA was applied in the 1700–650 cm^{-1} IR region. Full Cross-validation method, Singular Value Decomposition (SVD) algorithm, and Hotelling's T-Squared statistics were applied to the model, and the results were shown as scores and loadings plots.

HCA relies on assessing spectral similarities or distances. The hierarchical cluster algorithm operates as follows: (1) it amalgamates the two spectra with the highest similarity, signifying the smallest spectral distance, into a cluster, (2) it computes distances between this newly formed cluster and all other spectra, (3) it once again merges the two spectra with the smallest distance, whether they are two spectra, a spectrum and a cluster, or two clusters, into a novel cluster, (4) it recalculates the distances between this new cluster and all the remaining spectra, be they spectra or clusters, (5) the procedure is iteratively repeated until only one large cluster remains [25]. Here, HCA analysis was applied through OPUS 5.5 software from Bruker as described before [25]. In brief, the second derivative was computed for each sample within the 1700–1000 cm^{-1} range, and vector normalization was applied across the investigated wavenumber spectrum. The spectral distances were measured using Pearson's correlation coefficients, and cluster analysis was performed based on Euclidean distances. Dendrograms were constructed using the Complete Linkage algorithm.

IR spectroscopy experiments were conducted with two biological replicates, with three samples collected from each replicate.

2.6. Statistical analysis

All data are presented as the means ± standard error of the mean (SEM). GraphPad Prism v8 (GraphPad, La Jolla, CA, USA) software was used for the preparation of the graphs and statistical analysis. The experiments were repeated at least with two biological replicates and *t*-test was used to compare the results. Differences were considered to be significant when the *p*-value was lower than 0.05. The degree of significance was denoted as $*p \leq 0.05$, $**p \leq 0.01$, $***p \leq 0.001$, and $****p \leq 0.0001$.

3. Results and discussions

3.1. DMSO treatment causes more negative membrane potential

Bacteria are electrically powered organisms; their cells maintain an electrical potential across the plasma membrane. This electrical potential, known as the membrane potential or transmembrane voltage, serves as a source of free energy that enables cells to carry out essential biological processes [26,27]. In recent years, there has been a growing recognition of the dynamic nature of bacterial membrane potential which has been associated with various physiological processes and cell behaviors, including metabolic coordination [26].

Studies with the eukaryotic membranes have shown that DMSO can facilitate the passage of smaller molecules and ions and also larger molecules that would otherwise be unable to cross the membrane in the absence of DMSO [28]. Considering its well-known membrane permeability-enhancing effect as well as interaction with cellular membranes [29], we asked whether DMSO affects the membrane potential. As mentioned in the Materials and Methods section, $DiOC_2$ generates green fluorescence when inside bacterial cells. Nevertheless, an enhanced membrane potential triggers a rise in the dye's concentration within the cytoplasm, inducing aggregation of the dye molecules and thereby causing a shift toward red fluorescence emission. Fig. 1a shows the decrease in the percentage of green fluorescence (FL1) and an increase in the red fluorescence (FL3) upon DMSO treatment in a dose-dependent manner (left panel). The combined histograms are given in Fig. 1b and the FL3/FL1 ratio, which shows an increase in the DMSO-treated bacteria compared to untreated control, is presented in Fig. 1c. This outcome illustrates a more negative membrane potential compared to the resting state in DMSO-treated bacteria. Such a phenomenon occurs when there is an increased efflux of positively charged ions or a decreased influx of positively charged ions across the cell membrane [30]. The altered potential can be caused by the physicochemical changes induced by DMSO, such as:

(i) DMSO's influence on ion transport: It was previously reported that DMSO generates transient water pores on the membrane by causing the hydrophilic portions of the lipid headgroups to protect the hydrophobic tails from direct contact with water at the edge of the bilayer [6,15,31,32]. He et al. claimed that the formation of these pores significantly lowers the energy barriers for ions to pass through the membrane. This enables ions to move across the membrane, preventing unfavorable interactions with the hydrophobic lipid tails within the membrane's interior [16]. Gurtovenko and Vattulainen used atomic-scale molecular dynamics simulations to address ion leakage through transient water pores in phospholipid membrane models. The authors proposed that the permeation of ions through the pore is influenced by ion type, likely due to variations in the energy barriers for ion permeation through the pore. In bilayer systems containing NaCl, Na^+ ions were expected to encounter a lower potential barrier for permeation compared to Cl^- ions. However, the significant interaction of Na^+ ions with lipid headgroups led to a slowed permeation rate through hydrophilic water pores. As a result, both Na^+ and Cl^- ions were observed to pass through the membrane at similar rates. Conversely, in the context of KCl, there was a distinct preference for the membrane to allow the passage of K^+ ions over Cl^- ions. Around three-quarters of all leaked ions were K^+ ions. This selectivity mainly arises from the weak interaction between K^+ ions and the carbonyl regions of phospholipids [33]. More recently Xiang et al. showed that in the human monocytic cell line THP-1, DMSO concentrations between 0.5 and 10 % (*v*/v) resulted in cellular K^+ efflux [34]. In strong concurrence with these findings, the observed alterations in bacterial membrane potential here can be attributed to the ion flow facilitated by the water pores induced by DMSO. These water pores enable the passage of certain ions that contribute to hyperpolarization.

(ii) Alterations in membrane permeability: DMSO can change the arrangement of lipid molecules in the cell membrane, potentially enhancing its permeability [29]. This alteration can result in changes in the movement of ions in and out of the cell.

(iii) Interaction of DMSO with membrane components: DMSO's interaction with membrane lipids and proteins can affect the arrangement and activity of ion transport proteins, potentially leading to changes in ion movement and subsequent hyperpolarization.

(iv) Localization of DMSO in the interfacial region: DMSO molecules in the interfacial region may reduce the activation energy required for passive diffusion of solutes through biomembranes, further influencing the polarization state [35]. Additionally, changes in lipid and protein content and properties, as discussed in this study, can also contribute to alterations in ionic flux through the membrane by affecting membrane characteristics.

(v) DMSO's impact on electron transport and redox processes: Our previous findings and those of others have indicated DMSO's effect on redox processes [7,14,36]. Such action can potentially disrupt the equilibrium of ions and charges across the membrane, which could lead

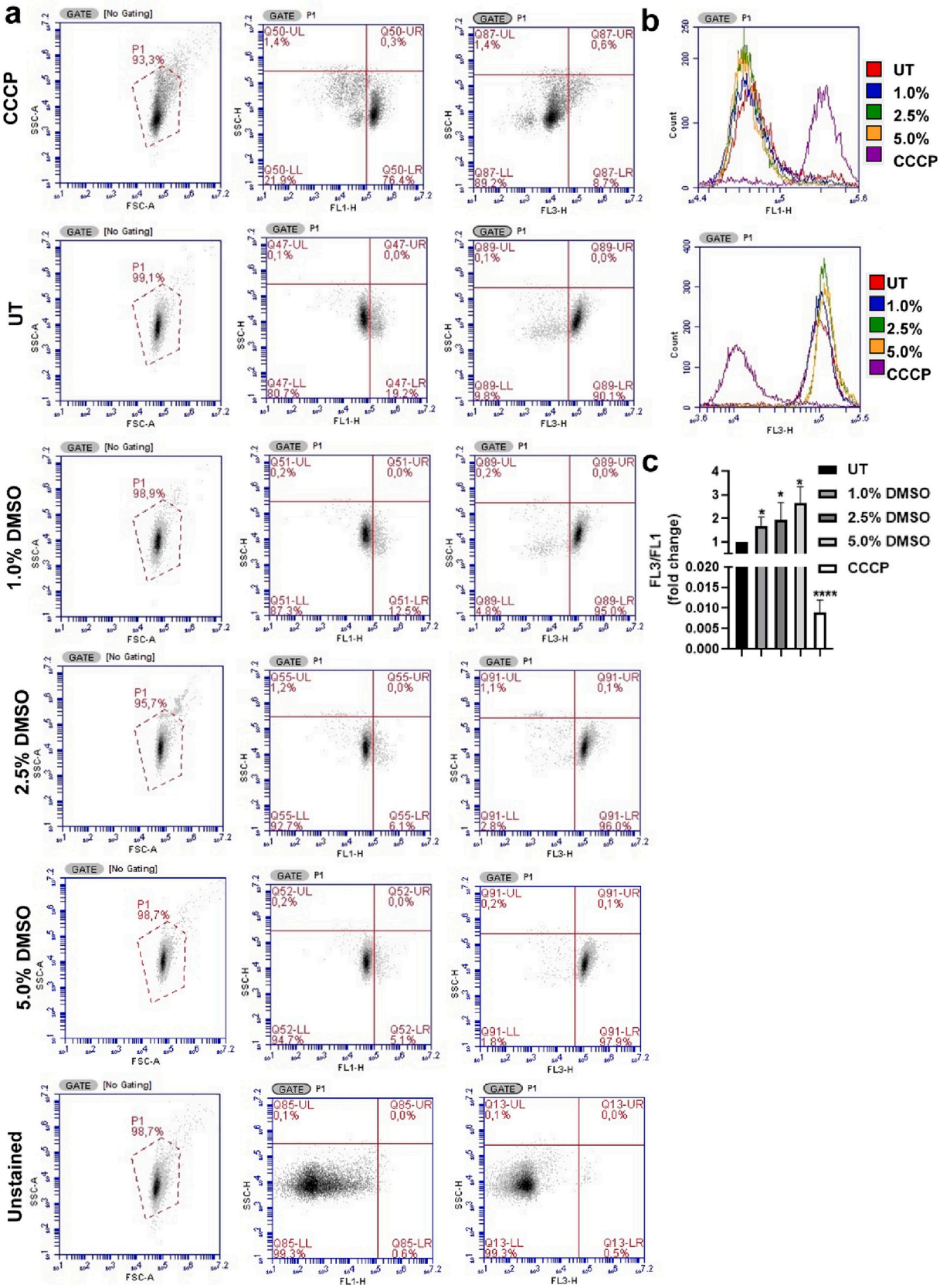

Fig. 1. DMSO treatment changes bacterial membrane potential. (a) Cell populations (P1) are presented on the left and the dot-plot analysis for FL1 and FL3 (in P1) are shown in the middle and right panels, respectively. CCCP-treated cells were used for gating (on the top) and unstained cells were used as negative control (on the bottom). (b) Histogram analysis for the FL1 ve FL3 are presented. Dot plots and histograms are representative. (c) The bar graph shows the ratio of FL3% positive cells to FL1% positive cells as fold change with respect to untreated (UT) control cells. *t*-test was applied for comparisons between the UT and the treatment groups.

to shifts in electrochemical gradients, thereby contributing to membrane hyperpolarization. Moreover, DMSO-dependent modulations in the expression of genes involved in metabolism, including glycolysis and cofactor biosynthesis may also play a role in the observed changes in ion balance [14].

Besides, this effect can also be attributed to DMSO-induced modifications in ion channels. Bacterial cell membranes have ion channels that regulate the flow of ions in and out of the cell [27]. By changing the membrane dynamics, DMSO could modulate the activity of these ion channels, affecting the movement of ions across the membrane. Depending on the specific ions and channels involved, this could result in an increased net movement of positive or negative ions, leading to membrane hyperpolarization. Previously, we demonstrated that low-dose (1.0 % and 2.5 %) DMSO treatment induces alterations in gene expression in *E. coli* [14]. Analysis of this publicly available transcriptome data (Bioproject number: PRJNA777047) revealed a down-regulation of *kdpB* (NP_415225) transcription with a $\log_2$-fold change of 1.808 ($p = 0.91$). For 2.5 % DMSO treatment, the $\log_2$-fold reduction is 1.246 ($p = 0.85$). KdpFABC functions as an oligomeric K^+ transport complex in prokaryotes, playing a crucial role in maintaining ionic homeostasis during stressful conditions. This active transport system is pivotal for maintaining internal K^+ concentrations, which are essential for membrane potential control. The complex consists of a channel-like subunit (KdpA) categorized under the superfamily of K^+ transporters, while KdpB serves as the pump-like subunit from the superfamily of P-type ATPases [37]. Thus, changes in the electrochemical potential of the membrane might not solely stem from DMSO-induced physicochemical alterations but could also be influenced by DMSO's impact on gene expression.

3.2. DMSO treatment changes the electrochemical property of the cell surface

The net charge on the cell surface can be evaluated by examining the Zeta Potential (ZP), the electric potential difference at the hydrodynamic slipping surface and the stationary fluid layer adhering to the cell surface. ZP is significant in maintaining cellular function and offers valuable insights into cell surface properties [38]. For instance, agglutination is enhanced when the zeta potential of red blood cells decreases (less negative zeta potential) [39]. The unicellular nature of bacteria, coupled with the absence of internal membrane-bound compartments, underscores the critical role of the interface formed between the outer cell envelope and the external environment in governing bacterial functionality. This external cell surface acts as a conduit for exchanges, adhesion processes, and interactions with immune factors, actively contributing to the cell's metabolic state. Consequently, the surface characteristics determine the overall polarity required to establish and maintain the surface's essential hydrophilicity for optimal cellular function [40]. Bacterial surface properties also become highly significant when examining the interaction between bacteria and different substances. Surface charge is typically the primary consideration when investigating the binding process. Thus, analyzing ZP can offer a powerful means to comprehend how antimicrobial agents, such as peptides and nanoparticles, interact with bacteria, particularly during their initial attachment phase, which is pivotal for their effectiveness. This approach provides valuable insights into the potential targeting of the bacterial membrane by these agents as part of their biological activity. Insights gleaned from investigations into alterations in ZP and dynamic molecular simulations indicate that antimicrobial agents accumulate on the bacterial surface in a charge-dependent manner, inducing changes in ZP that yield information about the bacterial-compound interaction [40]. Given DMSO's water-soluble nature and amphiphilic properties, previous studies have demonstrated its strong interaction with the membrane surface [28,29,35,41]. Consequently, our objective was to investigate how DMSO impacts the surface potential of bacteria by employing ZP measurements, a fast, straightforward, and cost-effective analytical method.

In the context of most bacteria, the surface carries a negative net charge that is balanced by oppositely charged counter ions in the surrounding environment [38]. As shown in Table 1 and Fig. 2, the ZP of the untreated *E. coli* was found to be -40.44 ± 3.3095 mV similar to the previous finding [38]. Treatment with non-growth inhibitory concentrations of DMSO (1.0 % and 2.5 %) resulted in a more negative ZP compared to the untreated control. On the other hand, 5.0 % DMSO-treated *E. coli* exhibited a significantly less negative ZP compared to the low-dose treated (1.0 % and 2.5 %) bacteria and tended to be less negative than the untreated control group ($p = 0.07$).

DMSO's impact on the overall charge distribution of the bacterial surface can be the key factor in altering the ZP. DMSO forms the intermolecular hydrogen bonding with water via the weak proton acceptor group of S = O [42]. DMSO can also interact strongly with polar lipids and proteins through the formation of hydrogen bonds [35]. Thus, since it is known that DMSO creates a positive charge on S and a negative charge on O through charge delocalization, the more negative ZP could be a result of the interaction between the outer layer and DMSO by $S(\delta^+)$ [43]. Of note, this interaction can also be correlated with the permeabilization effect of DMSO: DMSO acts indirectly in altering lipid order via an impact on the displacement of water from the polar lipids (like polar residues in lipopolysaccharide) and proteins [35]. Conversely, *E. coli* exposed to 5.0 % DMSO displayed a markedly reduced negative ZP compared to the bacteria subjected to lower doses (1.0 % and 2.5 %) and exhibited a trend toward being less negatively charged than the untreated control group. Klodzinska and her colleagues demonstrated in their study on *E. coli* and *Staphylococcus aureus* that the surface charge of dead cells is comparatively less negative than that of viable cells [44]. In line with these findings, Szumski et al. [45] and Ranawat et al. [46] have also claimed that the surface charge becomes less negative in dead bacteria. Thus, at 5.0 % DMSO, disarrangement of surface charges can result in disruption of the barrier function of the cell membrane [40] and the less negative ZP can be a result of decreased viability due to the induction of membrane injury and/or reduction in viability.

DMSO-induced modifications in the cell membrane, including alterations in the biochemical structures (such as lipopolysaccharides, flagellar proteins, fimbrial proteins, and curli proteins) and variations in the composition of lipids, proteins, and functional groups, can significantly influence surface morphology, resulting in a shift in ZP [14,40,47]. Alterations in ZP carry implications for bacterial behavior, ultimately affecting bacterial physiology and interactions between cells. This phenomenon has been demonstrated in *Staphylococcus aureus*, where biofilm-detached cells were less negatively charged than their planktonic counterparts [40]. It is noteworthy that low-dose DMSO treatment (<2 % *v*/v) has been linked to a reduction in biofilm formation in various bacterial species [10]. In our previous study, transcriptome analysis further revealed a significant down-regulation of genes related to biofilm formation in *E. coli* treated with 1.0 % and 2.5 % DMSO compared to untreated bacteria [14]. Besides, DMSO-induced changes in bacterial surface characteristics and variations in surface charge can influence bacterial responses to different environmental conditions. This includes their interactions with membrane-acting agents, such as certain groups of antimicrobial agents, resulting in synergistic or antagonistic effects depending on the bacterial species and the specific membrane-acting agent [10,40].

Table 1
Zeta potentials of untreated and DMSO-treated bacteria.

Treatment	Zeta potential (mV ± STD)
Untreated-UT (control)	−40.44 ± 3.3095
1.0 % DMSO	−43.2 ± 0.892
2.5 % DMSO	−45.27 ± 0.96
5.0 % DMSO	−35.54 ± 6.52

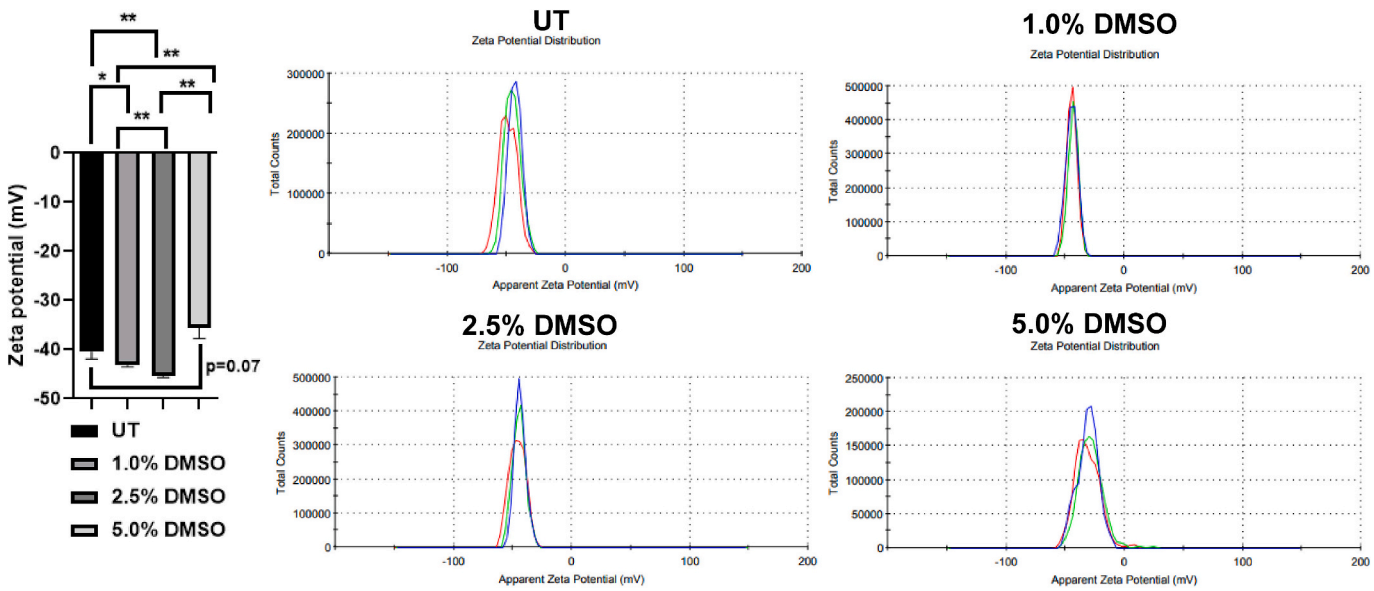

Fig. 2. DMSO treatment affects the surface charge in bacteria. Results of ZP measurements are presented on the left and the representative records for the ZP measurements of DMSO-treated and untreated (UT) samples are shown on the right. *t*-tests were applied for comparisons between the treatment groups and the UT and among the treatment groups as specified.

3.3. Chemometric tools show the distinction between DMSO-treated bacteria from the untreated control

A substantial number of studies with both model and biological membranes revealed that DMSO affects the structural properties of the membranes [28,29,35,48,49]. Taking a comprehensive perspective, we aimed to investigate the effects of DMSO treatment on cellular lipid, protein, and nucleic acid structure and content. We employed Fourier-transform infrared (FT-IR) spectroscopy and chemometrics to contribute to a better understanding of DMSO's broader biological effects, which can potentially influence various cellular processes.

First, PCA was applied to spectral data to investigate whether DMSO-treated cells can be distinguished from untreated control cells. In the fingerprint region (1700–650 cm^{-1}) of DMSO-treated and untreated (UT) control bacteria, the PCA scores plot showed a sharp separation (Fig. 3a), and PC-1 made the highest contribution (98 %) to intergroup variation. The loading plot in Fig. 3b reflects the spectral position of the changes that occur with the positive Eigenvector values. The discriminators on the loading plot prove that the spectral differences between the control and DMSO-treated bacterial groups mainly happen in the fingerprint spectral region. These positive discriminants show their effects on principal component scores and are, therefore, the essential variables underlying the differentiation of groups from one another. The dendrogram of HCA in the 1700–1000 cm^{-1} spectral region (Fig. 3c) shows that the bacterial groups are completely separated from each other with a heterogeneity value >1.0, revealing the dissimilarity between the groups [50].

3.4. Significant alterations in macromolecules arise in DMSO-treated bacteria

3.4.1. Alterations in lipids

Considering DMSO's capability to influence lipid bilayers and potentially impact membrane properties, we analyzed DMSO-triggered changes in cellular lipid composition from FTIR spectra. Fig. 4a, b and c show the intensities (%) for olefinic (~3016 cm^{-1}), CH_2 symmetric (~2852 cm^{-1}), and CH_2 anti-symmetric (~2920 cm^{-1}) bands, respectively [7]. The intensity of the olefinic (=CH) band, which arises from the unsaturated lipids [51,52], significantly decreased with 2.5 % and 5.0 % DMSO treatment and the intensities of the bands assigned for the saturated lipid bands (anti-symmetric and symmetric vibration of CH_2 groups) were also diminished with DMSO treatment in a dose-dependent manner. Another significant peak for lipid analysis falls within the 1725–1740 cm^{-1} wavenumber range corresponding to the C = O stretches of ester functional groups found in lipid triglycerides and fatty acids [53]. This peak serves as an indicator of total lipids [54]. DMSO-related changes in the intensity and the wavenumber of lipid carbonyl band, detected around 1735 cm^{-1}, are given in Fig. 4d. The highest "unsaturation index" which is characterized by taking the ratio of 3016 cm^{-1} (olefinic band) to 1735 cm^{-1} (lipid carbonyl band) was calculated in the samples treated with 1.0 % DMSO, indicating a high content of unsaturated fatty acids [54] (Fig. 4e). A trend toward a higher degree of unsaturation was still evident in the samples treated with 2.5 % DMSO, but this effect was no longer observed in the bacteria treated with 5.0 % DMSO. An increase in membrane unsaturation, which results from elevated levels of unsaturated fatty acids, leads to enhanced membrane fluidity, which is vital for various cellular processes. [55]. This phenomenon happens due to the abundance of cis double bonds in the neighbor hydrocarbon chains (fatty acid tails), generating steric hindrance to each other. Thus, a high level of unsaturated lipids at 1.0 % and 2.5 % DMSO concentrations can increase the fluidity of the membrane's hydrophobic core [6], but the reversal of this effect at a 5.0 % DMSO concentration may indicate a survival response. Showing structural alterations [56], the significant increase in the wavenumber of the ester carbonyl stretching band in the samples treated with 5 % DMSO (Fig. 4d, right panel) also supports this suggestion: as previously observed in mammalian epithelial cells, when bacteria are exposed to higher DMSO concentrations, the cells may alter the lipid composition through a negative feedback mechanism to maintain cellular homeostasis [7]. In summary, the FT-IR spectral results indicate that even at non-growth inhibitory concentrations, DMSO reduces cellular lipid content. This observation aligns with previous studies. For instance, DMSO treatment (≥10 % *v*/v) of the 3T3-L1 murine preadipocyte cell line, a model for lipid metabolism studies, resulted in reduced lipid content, as measured by the oil red O assay [57]. Additionally, another study showed that 2 % (*v*/v) DMSO treatment led to decreased cellular cholesterol levels in human skin-isolated fibroblasts [58] consistent with our earlier findings using human colon cancer cell lines where DMSO was applied at concentrations of 0.5–1.5 % v/v [7].

The phospholipid bilayer, comprising different lipid classes, imparts

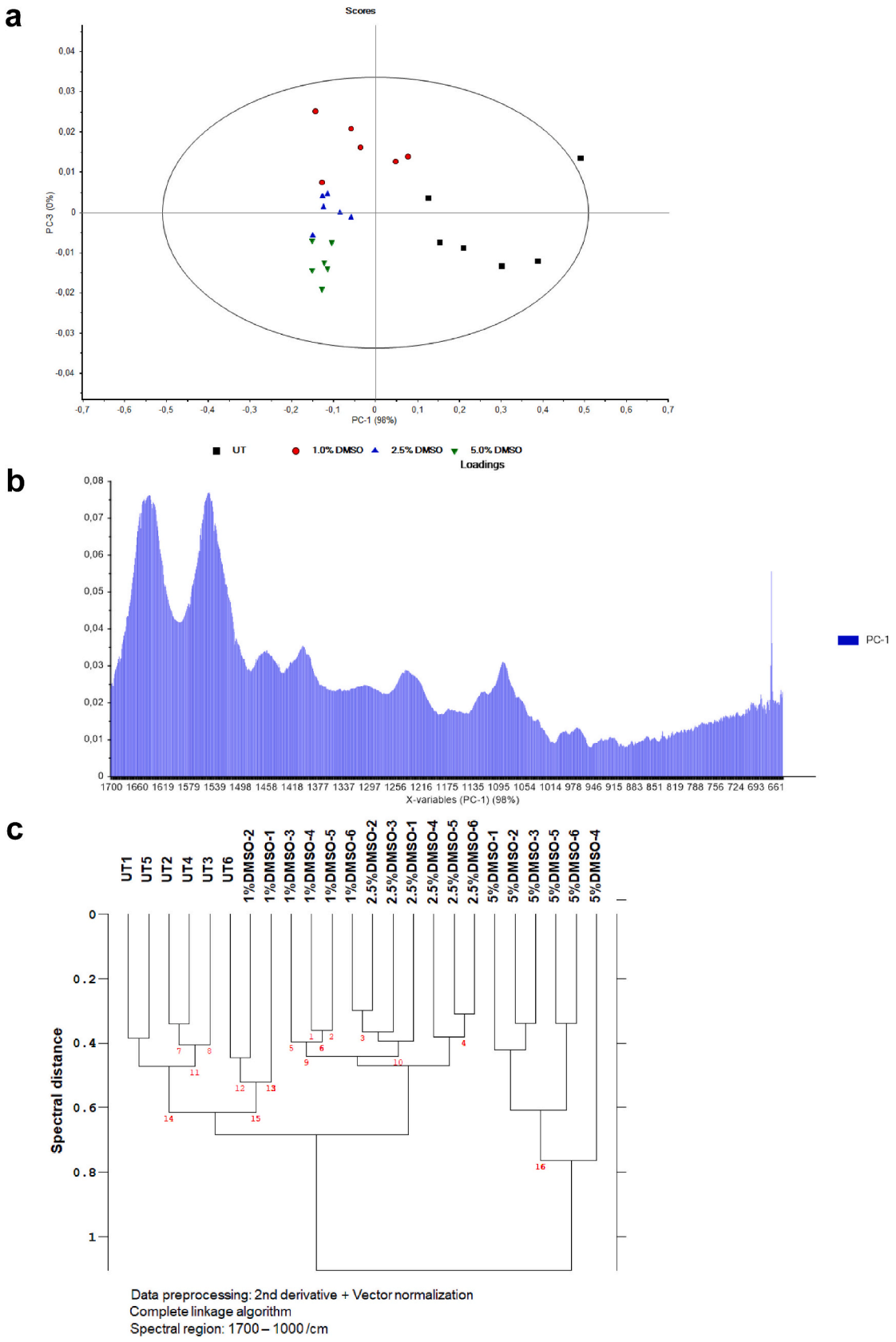

Fig. 3. Spectral data analyses reveal a well separation of low-dose DMSO-treated bacteria from untreated (UT) control cells. (a) PCA model and (b) loadings plot were obtained in the spectral range of 1700–650 cm^{-1}. (c) HCA of the samples in the spectral range of 1700–1000 cm^{-1} is shown.

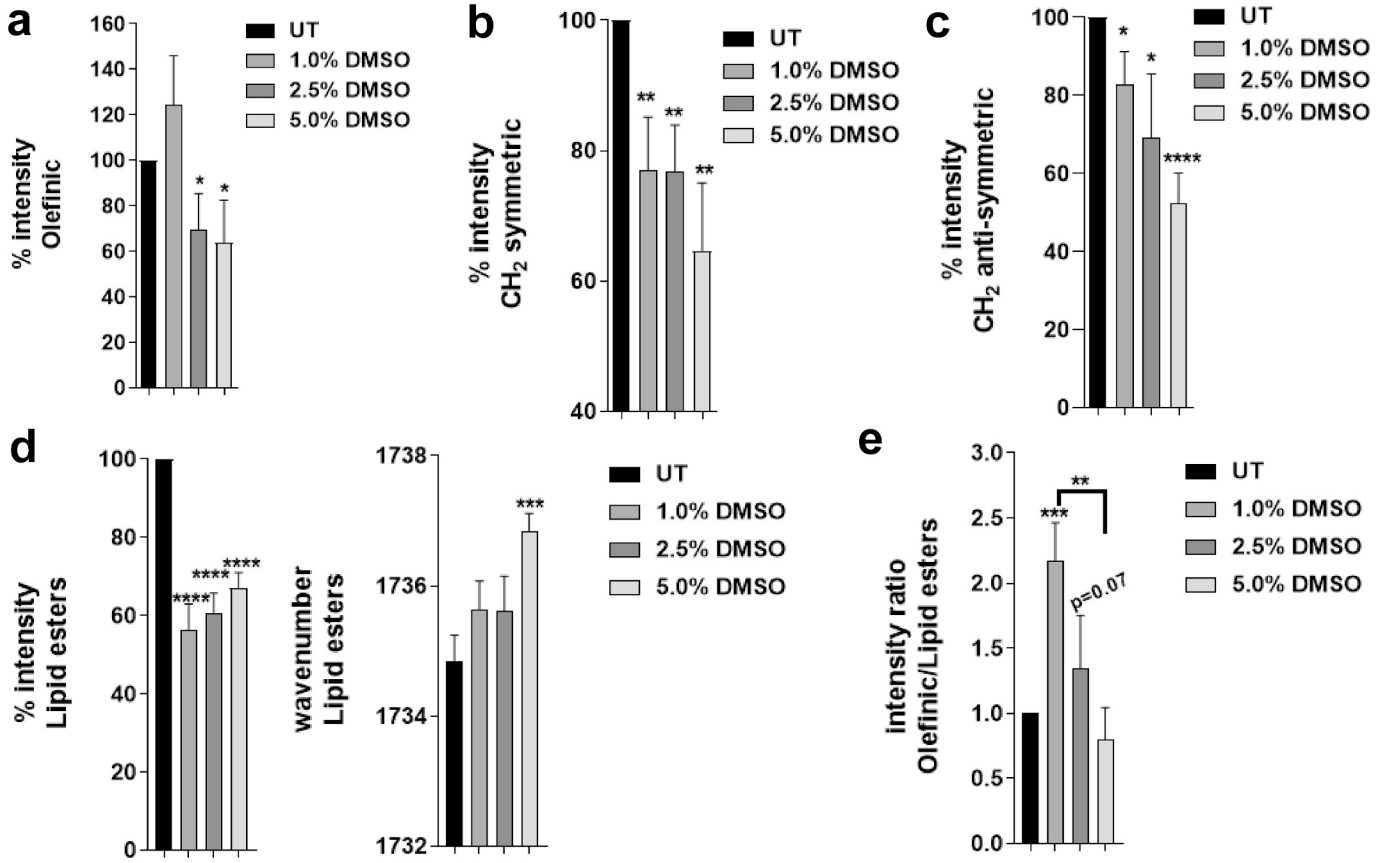

Fig. 4. IR spectrum indicates DMSO-driven changes in bacterial lipid content and structure. The band intensities for (a) olefinic, (b) CH_2 symmetric, and (c) CH_2 anti-symmetric are shown. The results presented as % change with respect to untreated control (UT). (d) The intensities of the carbonyl ester band (with respect to untreated control) are shown on the left and the changes in the wavenumber of this band are presented on the right. (e) As a degree of unsaturation, the intensity ratio for the olefinic to carbonyl ester band is presented as fold changes with respect to the untreated control group. *t*-test was used for the comparison of untreated control bacteria with the DMSO treatment groups. When indicated, the statistic was applied between the treatment groups.

an asymmetric structure to the cell membrane, crucial for both its barrier function and various biological processes [59]. Extensive evidence from simulations and experiments demonstrates that DMSO primarily modifies membrane structure by affecting intermolecular interactions in lipid head groups [60] and by influencing hydration in interface and polar head regions [59,61]. As a result, DMSO can modulate the membrane's structure or disrupt its integrity, increasing permeability, causing lipid leakage, and ultimately resulting in reduced total lipid content and membrane loosening and thinning, even at low concentrations in biological systems [6,28,61]. Furthermore, here we demonstrate that DMSO not only decreases the total lipid amount but also leads to a structural reconfiguration of cellular lipids. Consequently, DMSO-induced alterations in lipid structure and composition may impact membrane properties such as fluidity and permeability, as well as cellular function and behaviors. It is worth noting that changes in lipid content and composition due to DMSO treatment can also be attributed to the modulation of genes involved in cellular lipid metabolism (lipid synthesis or degradation) [14]. The lipid content reduction in bacteria might be due to the downregulation of genes associated with lipid synthesis and/or the upregulation of genes involved in lipid catabolism. Notably, the KEGG pathway enrichment analysis of Differentially Expressed Genes (DEGs) after 1.0 % and 2.5 % DMSO treatment (Bioproject number: PRJNA777047) in *E.coli* revealed that, compared to the untreated control, DMSO treatment upregulated genes linked to fatty acid degradation and downregulated genes related to glycerophospholipid metabolism and lipopolysaccharide biosynthesis [14].

3.4.2. *Alterations in proteins*

To determine whether the cellular proteins are also influenced by the DMSO treatments, we analyzed the IR spectrum of amides, including amide I (1600–1700 cm^{-1}) and amide II (1510–1580 cm^{-1}) regions [62]. As seen in Fig. 5a (on the left), in a dose-dependent manner, DMSO treatment causes wavenumber shifts in amide I without affecting the band intensity (Fig. 5a, on the right). This shift can be interpreted as an indication of an increase in the energies of the C═O stretch (70–85 % of the potential energy) [63] which could be influenced by DMSO's charge delocalization involving S(δ^+) and O(δ^-) atoms. The energy of the amide I's vibration has been reported to be notably influenced by alterations in hydration patterns between the protein and water molecules [64] and shifts in the amide I frequency are commonly attributed to modifications in the protein's folding state or conformation [65] which has been explained with altered intermolecular interactions at the interface such as electrostatics, hydrogen bonding, hydrophobic interactions, van der Waals forces or the modified interfacial interactions with ions, solvent molecules and cosolutes [65]. Functional and structural stability of proteins requires a fine balance between the favorable internal interactions among residues of the protein and with solvent molecules. Thus, it can be suggested that DMSO can alter protein structure by perturbing the structure of water around the protein molecule. This leads to DMSO-induced changes in the protein folding [7]. Analysis of the wavenumber of the amide II band also revealed a shift in the wavenumber toward to higher frequency (Fig. 5b, on the left) in 5.0 % DMSO-treated samples, significantly. As stated previously, the frequency of the amide I band is known to strongly correlate with the secondary structural elements found in proteins. It is important to note

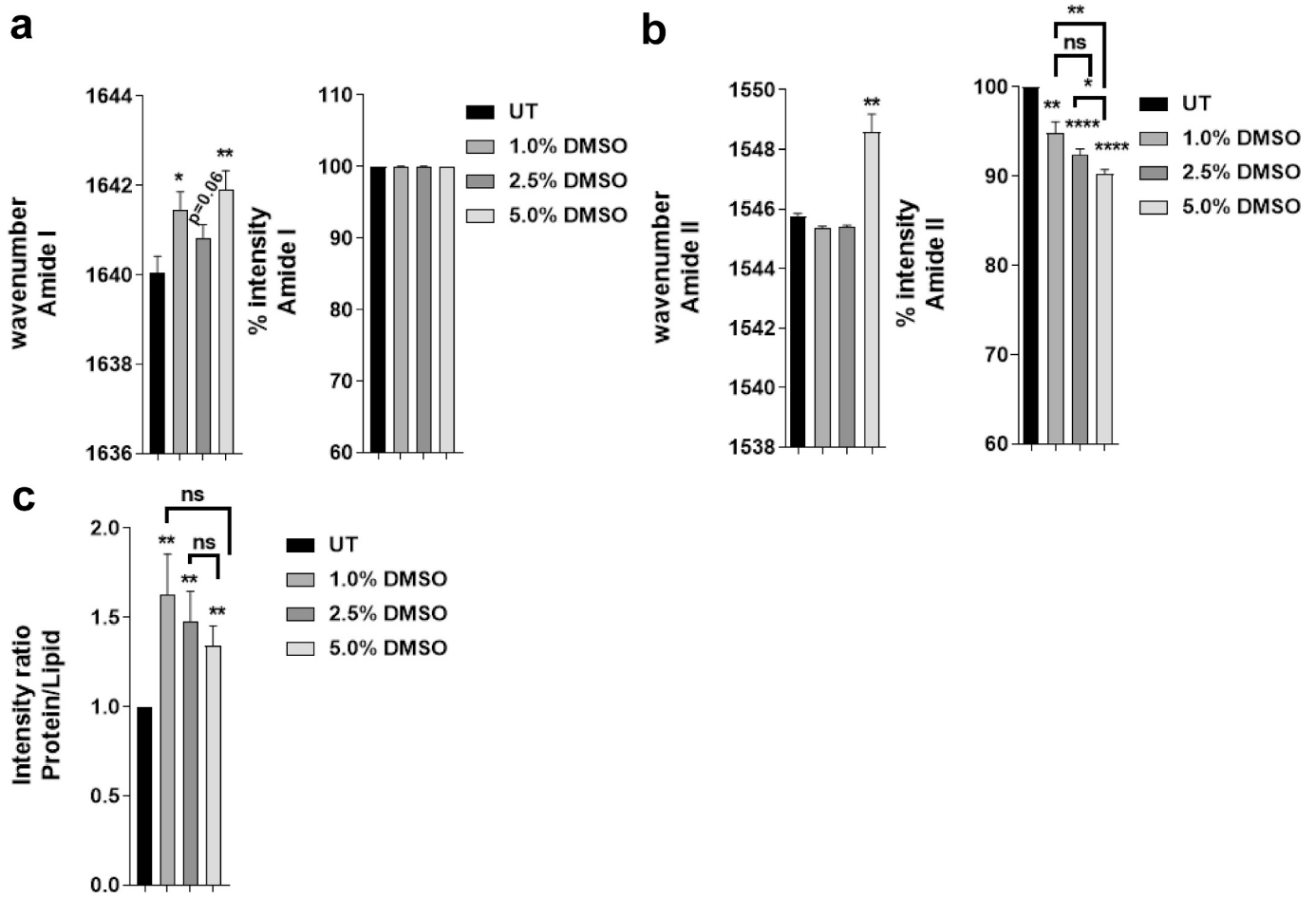

Fig. 5. Cellular proteins as well as protein-to-lipid ratio is affected by DMSO treatment. DMSO-driven changes in the wavenumbers and intensities (as % change with respect to the untreated control-UT) for the amide I (a) and amide II (b) bands are presented. (c) To assess the changes in the protein-to-lipid ratio, the sum of the intensities of amide I and amide II divided by the intensity of the carbonyl ester band and presented as fold change with respect to the untreated control. *t*-test was applied for comparison with the untreated control group or between the DMSO-treatment groups where indicated.

that the amide II band, primarily arising from in-plane NH bending (comprising 40–60 % of the potential energy), CN stretching vibration (contributing 18–40 %), and C—C stretching vibrations (about 10 %) [66], can also offer insights into secondary protein structure, although with lower sensitivity compared to amide I [67]. For example, shifts toward higher wavenumbers in the amide II band can be explained by weakened hydrogen bonds between peptide chains [68]. Therefore, when taken into consideration alongside the shift in the amide I band, the wavenumber shift in the amide II band can be proposed as a DMSO-induced structural alteration in proteins, particularly pronounced at higher DMSO concentration (5.0 % DMSO). In addition, a reduction in the intensity of the amide II band (Fig. 5b, on the right) is also likely to relate to conformational changes in the protein structure as discussed by Dickinson and High, previously [69]. The findings presented here align with previous research, including studies using human proteins, which demonstrated that relatively low concentrations of DMSO can alter protein properties in solution, leading to denaturation, aggregation, or degradation, and affecting the apparent binding properties of proteins [70]. In human epithelial cells, DMSO has been shown to modify the secondary structure of cellular proteins when used at concentrations between 0.5 % and 1.5 % *v*/v [7]. Furthermore, research with bacterial NAD^+ synthetase indicated that 2.5 % v/v DMSO alters dimer-monomer dynamics, possibly by weakening the hydrophobic effect for dimer formation without affecting the enzyme's catalytic activity [71]. These effects may result from perturbations in the structure of water around the protein molecule, leading to DMSO-induced protein denaturation or unfolding by disrupting hydrogen bonding and hydrophobic interactions that stabilize the protein's native structure [7]. Additionally, DMSO can directly interact with proteins, with varying interactions depending on the amino acids, amino acid side chains, and peptide groups present in the protein [72–74]. Given DMSO's widespread use as a solvent in various scientific fields, including toxicology, experimental pharmacology, antimicrobial screening, biochemical assays, and drug screening, structural changes induced by DMSO in proteins can influence the binding of small molecules or ligands to the proteins under investigation and directly impact the function of cellular proteins, potentially leading to experimental interpretation errors.

To maintain the stability and functionality of the membrane's bilayer structure, interactions between lipids and between lipids and membrane proteins play a crucial role [59]. Membranes are densely populated with proteins, and research has shown that changes in the protein-to-lipid ratio, or “crowding by membrane proteins,” can alter the stochastic characteristics of anomalous lateral diffusion in lipid membranes, resulting in multifractal, non-Gaussian, and spatiotemporally heterogeneous diffusion patterns [75]. Thus, changes in protein-to-lipid ratio may contribute to the effects of DMSO on membrane dynamics, including fluidity and permeability [76]. Considering this, we evaluated the relative intensity of protein to lipid using the FT-IR spectrum by dividing the sum of the intensities of amide I (around 1640 cm^{-1}) and amide II (around 1546 cm^{-1}), which collectively represent the total protein [77], by the intensity of the ester band around 1735 cm^{-1} [53]. A higher protein-to-lipid ratio was observed in the bacteria treated with

1.0 %. In contrast, a trend of decreasing protein-to-lipid ratio was observed with increasing DMSO concentrations (Fig. 5c), highlighting a stress response to restore homeostasis. Supporting this DMSO-driven stress phenomenon, KEGG pathway enrichment analyses of DEGs with 1.0 % and 2.5 % DMSO treatments in *E. coli* (publicly available RNA-seq data; Bioproject number: PRJNA777047) [14] reveal the differential expression of the genes that are members of the two-component regulatory system, such as sensor histidine kinases *dpiB*, *evgS*, *torS,* and DNA-binding transcriptional dual regulator *araC*, which enables bacteria to sense, respond, and adapt to changes in their environment or intracellular state [78].

3.4.3. Alterations in nucleic acids

We have previously illustrated that non-growth inhibitory concentrations of DMSO (1.0 % and 2.5 %) lead to a reduction in cellular nucleic acid content and induce structural alterations in nucleic acids [14]. Here, we also evaluated how the slight growth inhibiting DMSO concentration (5.0 %) affected the cellular nucleic acids (Fig. 6) by analyzing the PO_2 anti-symmetric band from the absorbance spectrum located between 1242 and 1238 cm^{-1} (assigned to total nucleic acids) [7,14]. The results show a significant decrease in the cellular nucleic acid in bacteria subjected to DMSO, along with a significant shift in the wavenumber of PO_2 indicating structural modifications of nucleic acids. It should also be emphasized that treatment with 5.0% DMSO, despite exerting slight growth inhibition, induces similar effects on nucleic acids as observed with the non-growth inhibitory concentrations [14].

DMSO, through the formation of hydrogen bonds with DNA bases, has the potential to induce changes in helix conformation, potentially affecting DNA replication and transcription processes and resulting in an overall decrease in cellular nucleic acid content. Recent research using circular and linear DNA supports this notion, indicating that treatment of DNA with DMSO causes a reduction in particle size and the mean dimension of DNA with increasing DMSO concentration [79]. Physical interactions between DMSO and nucleic acids are further supported here by changes in the anti-symmetric PO_2 wavenumber. In addition, it is important to mention that DMSO can induce epigenetic changes, potentially leading to structural modifications in nucleic acids [12,14,80,81], which can, in turn, influence the dynamics of transcription and gene expression [14].

4. Conclusion

DMSO's interaction with biological membranes and cellular macromolecules presents a complex and multifaceted phenomenon. These interactions can manifest as direct interactions, involving the physical engagement of DMSO with proteins, nucleic acids, and lipids, or they can occur indirectly by altering membrane properties and influencing the transport of ions, nutrients, and other crucial molecules on which macromolecules depend for their functions. These collective influences can alter the cell's electrochemical properties, potentially impacting a diverse range of cellular processes, such as cell signaling, intercellular communication, and gene expression. Consistent with the spectrochemical analysis presented in this study, GO enrichment data on DEGs indicate that “Biological Process” and “Cellular Component” are the most significantly over-represented categories in response to low-dose (1.0 % and 2.5 %) DMSO treatment of *E. coli*. Additionally, KEGG pathway enrichment analyses of DEGs revealed that DMSO treatment predominantly influences the expression of genes involved in metabolism, aligning with the significant spectral alterations observed in cellular biomolecules, which are the products of metabolic reactions [14]. Furthermore, the effects of DMSO appear to be target-dependent, contingent upon the specific gene, protein, and cellular model under investigation [70,82].

It is widely acknowledged that in numerous cases, the biological and therapeutic effects of DMSO are attributed to its capacity to act as a carrier, facilitating the transport of drugs into the cell [29]. As a result,

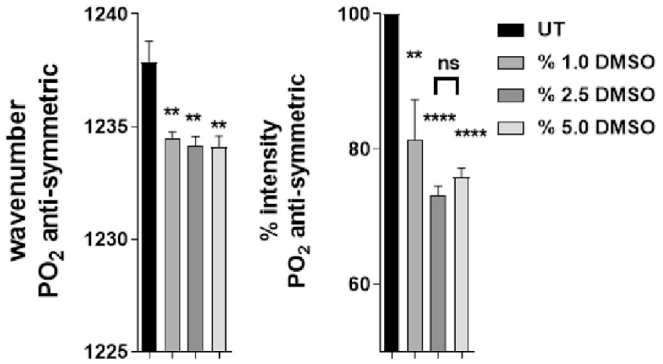

Fig. 6. Both non-growth inhibitory and growth inhibitory concentrations of DMSO affect cellular nucleic acids. In DMSO-treated bacteria, changes in the wavenumber (on the left) and the intensity of the PO_2 anti-symmetric band (on the right; represented as % change with respect to the untreated control-UT) are shown. *t*-test was used for the comparison of the untreated group with the DMSO treatment groups. When indicated, the statistic was conducted between the treatment groups.

DMSO's interactions with macromolecules, which may involve direct binding to functional groups and the exertion of effects on cellular processes, can be leveraged by researchers to explore and modulate cellular functions or to enhance the delivery of bioactive compounds. On the other hand, when utilizing DMSO to enhance the solubility and delivery of bioactive compounds, researchers must be mindful of the potential manipulation of cellular molecules and functions by DMSO.

Funding

This work was supported by The Scientific and Technological Research Council of Turkey, grant no 120Z017 (to STÇ) and Bilecik Şeyh Edebali University, Scientific Research Fund, Project no 2017–02. BŞEÜ.04–04 (to RG).

Author contributions

STÇ designed the study and carried out the experiments and analyzed the results, except for the FT-IR experiments which were performed by RG. STÇ wrote the manuscript. The final manuscript has been read and approved by both authors.

CRediT authorship contribution statement

Sinem Tunçer Çağlayan: Conceptualization, Data curation, Formal analysis, Funding acquisition, Investigation, Methodology, Project administration, Resources, Software, Supervision, Validation, Visualization, Writing – original draft, Writing – review & editing. **Rafig Gurbanov:** Data curation, Writing – review & editing.

Declaration of competing interest

The authors declare that they have no affiliations with or involvement in any organization or entity with any financial interest in the subject matter or materials discussed in this manuscript.

Data availability

Data will be made available on request.

Acknowledgments

The authors thank the Biological Sciences Department of Middle East Technical University for the flow-cytometry facility and Molecular

Biology and Genetics Department, Biotechnology Application and Research Center, and Chemistry Department of Bilecik Şeyh Edebali University for sharing the laboratory facilities.

References

[1] S.W. Jacob, J.C. De La Torre, Dimethyl Sulfoxide (DMSO) in Trauma and Disease, 2015, https://doi.org/10.1201/b18275.

[2] R. Brito, G. Silva, T. Farias, P. Ferreira, S. Ferreira, Standardization of the safety level of the use of DMSO in viability assays in bacterial cells, in: Proc. MOL2NET 2017, Int. Conf. Multidiscip. Sci, 3rd Ed, MDPI, Basel, Switzerland, 2017, p. 4980, https://doi.org/10.3390/mol2net-03-04980.

[3] S. Chetty, F.W. Pagliuca, C. Honore, A. Kweudjeu, A. Rezania, D.A. Melton, A simple tool to improve pluripotent stem cell differentiation, Nat. Methods 10 (2013) 553–556, https://doi.org/10.1038/nmeth.2442.

[4] J. Li, C. Narayanan, J. Bian, D. Sambo, T. Brickler, W. Zhang, S. Chetty, A transient DMSO treatment increases the differentiation potential of human pluripotent stem cells through the Rb family, PLoS One (2018), https://doi.org/10.1371/journal.pone.0208110.

[5] R. Pal, M.K. Mamidi, A.K. Das, R. Bhonde, Diverse effects of dimethyl sulfoxide (DMSO) on the differentiation potential of human embryonic stem cells, Arch. Toxicol. (2012), https://doi.org/10.1007/s00204-011-0782-2.

[6] A.A. Gurtovenko, J. Anwar, Modulating the structure and properties of cell membranes: the molecular mechanism of action of dimethyl sulfoxide, J. Phys. Chem. B 111 (2007) 10453–10460, https://doi.org/10.1021/jp073113e.

[7] S. Tunçer, R. Gurbanov, I. Sheraj, E. Solel, O. Esenturk, S. Banerjee, Low dose dimethyl sulfoxide driven gross molecular changes have the potential to interfere with various cellular processes, Sci. Rep. 8 (2018), https://doi.org/10.1038/s41598-018-33234-z.

[8] A.S. McKim, R. Strub, Advances in the regulated pharmaceutical use of dimethyl sulfoxide USP, Pharm. Technol. Eur. (2016) 30–35.

[9] K. Marren, Dimethyl sulfoxide: an effective penetration enhancer for topical administration of NSAIDs, Phys. Sportsmed. (2011), https://doi.org/10.3810/psm.2011.09.1923.

[10] K. Summer, J. Browne, M. Hollanders, K. Benkendorff, Out of control: the need for standardised solvent approaches and data reporting in antibiofilm assays incorporating dimethyl-sulfoxide (DMSO), Biofilm 4 (2022) 100081, https://doi.org/10.1016/j.bioflm.2022.100081.

[11] T. Kelava, I. Čavar, F. Čulo, Biological actions of drug solvents, Period. Biol. (2011) 311–320.

[12] M. Verheijen, M. Lienhard, Y. Schrooders, O. Clayton, R. Nudischer, S. Boerno, B. Timmermann, N. Selevsek, R. Schlapbach, H. Gmuender, S. Gotta, J. Geraedts, R. Herwig, J. Kleinjans, F. Caiment, DMSO induces drastic changes in human cellular processes and epigenetic landscape in vitro, Sci. Rep. (2019), https://doi.org/10.1038/s41598-019-40660-0.

[13] M. Awan, I. Buriak, R. Fleck, B. Fuller, A. Goltsev, J. Kerby, M. Lowdell, P. Mericka, A. Petrenko, Y. Petrenko, O. Rogulska, A. Stolzing, G.N. Stacey, Dimethyl sulfoxide: a central player since the dawn of cryobiology, is efficacy balanced by toxicity? Regen. Med. 15 (2020) 1463–1491, https://doi.org/10.2217/rme-2019-0145.

[14] S. Tunçer, R. Gurbanov, Non-growth inhibitory doses of dimethyl sulfoxide alter gene expression and epigenetic pattern of bacteria, Appl. Microbiol. Biotechnol. (2022) 299–312, https://doi.org/10.1007/s00253-022-12296-0.

[15] R. Notman, M. Noro, B. O'Malley, J. Anwar, Molecular basis for dimethylsulfoxide (DMSO) action on lipid membranes, J. Am. Chem. Soc. 128 (2006) 13982–13983, https://doi.org/10.1021/ja063363t.

[16] F. He, W. Liu, S. Zheng, L. Zhou, B. Ye, Z. Qi, Ion transport through dimethyl sulfoxide (DMSO) induced transient water pores in cell membranes, Mol. Membr. Biol. 29 (2012) 107–113, https://doi.org/10.3109/09687688.2012.687460.

[17] F. Ermawati, R. Sari, N. Putri, L. Rohmawati, D. Kusumawati, Z. Supardi Munasir, Antimicrobial activity analysis of *Piper betle* Linn leaves extract from Nganjuk, Sidoarjo and Batu against *Escherichia coli*, *Salmonella* sp., *Staphylococcus aureus* and *Pseudomonas aeruginosa*, J. Phys. Conf. Ser. 2021 (1951) 012004, https://doi.org/10.1088/1742-6596/1951/1/012004.

[18] A. Ishihama, Adaptation of gene expression in stationary phase bacteria, Curr. Opin. Genet. Dev. 7 (1997) 582–588, https://doi.org/10.1016/S0959-437X(97)80003-2.

[19] C.H. Lee, J.S.H. Oon, K.C. Lee, M.H.T. Ling, *Escherichia coli* ATCC 8739 adapts to the presence of sodium chloride, monosodium glutamate, and benzoic acid after extended culture, ISRN Microbiol. (2012), https://doi.org/10.5402/2012/965356.

[20] K.T. Militello, L. Finnerty-Haggerty, O. Kambhampati, R. Huss, R. Knapp, DNA cytosine methyltransferase enhances viability during prolonged stationary phase in *Escherichia coli*, FEMS Microbiol. Lett. (2020), https://doi.org/10.1093/femsle/fnaa166.

[21] K.T. Militello, R.D. Simon, M. Qureshi, R. Maines, M.L. Horne, S.M. Hennick, S. K. Jayakar, S. Pounder, Conservation of Dcm-mediated cytosine DNA methylation in *Escherichia coli*, FEMS Microbiol. Lett. 328 (2012) 78–85, https://doi.org/10.1111/j.1574-6968.2011.02482.x.

[22] W. Ng, Y.-P. Ting, Zeta potential of bacterial cells: effect of wash buffers, PeerJ Prepr. Open Acces (2016) 2–3, https://doi.org/10.7287/PEERJ.PREPRINTS.110V3.

[23] S. Tunçer, R. Gurbanov, A novel approach for the discrimination of culture medium from vascular endothelial growth factor (VEGF) overexpressing colorectal cancer cells, Turk. J. Biochem. (2020), https://doi.org/10.1515/tjb-2020-0058.

[24] R. Gurbanov, S. Tunçer, The use of Fourier-transform infrared spectroscopy to determine potential starch-based prebiotics 4 (2021) 22–30, https://doi.org/10.18016/ksutarimdoga.vi.742250.

[25] R. Gurbanov, M. Bilgin, F. Severcan, Restoring effect of selenium on the molecular content, structure and fluidity of diabetic rat kidney brush border cell membrane, Biochim. Biophys. Acta Biomembr. 2016 (1858) 845–854, https://doi.org/10.1016/j.bbamem.2016.02.001.

[26] J.M. Jones, J.W. Larkin, Toward bacterial bioelectric signal transduction, Bioelectricity (2021), https://doi.org/10.1089/bioe.2021.0013.

[27] J.M. Benarroch, M. Asally, The microbiologist's guide to membrane potential dynamics, Trends Microbiol. (2020), https://doi.org/10.1016/j.tim.2019.12.008.

[28] B. Gironi, Z. Kahveci, B. McGill, B.-D. Lechner, S. Pagliara, J. Metz, A. Morresi, F. Palombo, P. Sassi, P.G. Petrov, Effect of DMSO on the mechanical and structural properties of model and biological membranes, Biophys. J. 119 (2020) 274–286, https://doi.org/10.1016/j.bpj.2020.05.037.

[29] V.I. Gordeliy, M.A. Kiselev, P. Lesieur, A.V. Pole, J. Teixeira, Lipid membrane structure and interactions in dimethyl sulfoxide/water mixtures, Biophys. J. (1998), https://doi.org/10.1016/S0006-3495(98)77678-7.

[30] E.A.K. Warren, C.K. Payne, Cellular binding of nanoparticles disrupts the membrane potential, RSC Adv. 5 (2015) 13660–13666, https://doi.org/10.1039/C4RA15727C.

[31] A.A. Gurtovenko, J. Anwar, Ion transport through chemically induced pores in protein-free phospholipid membranes, J. Phys. Chem. B 111 (2007) 13379–13382, https://doi.org/10.1021/jp075631v.

[32] C.-Y. Cheng, J. Song, J. Pas, L.H.H. Meijer, S. Han, DMSO induces dehydration near lipid membrane surfaces, Biophys. J. 109 (2015) 330–339, https://doi.org/10.1016/j.bpj.2015.06.011.

[33] A.A. Gurtovenko, I. Vattulainen, Ion leakage through transient water pores in protein-free lipid membranes driven by transmembrane ionic charge imbalance, Biophys. J. 92 (2007) 1878–1890, https://doi.org/10.1529/biophysj.106.094797.

[34] Y. Xiang, M. Zhao, S. Sun, X.-L. Guo, Q. Wang, S.-A. Li, W.-H. Lee, Y. Zhang, A high concentration of DMSO activates caspase-1 by increasing the cell membrane permeability of potassium, Cytotechnology 70 (2018) 313–320, https://doi.org/10.1007/s10616-017-0145-9.

[35] Z.-W. Yu, P.J. Quinn, The modulation of membrane structure and stability by dimethyl sulphoxide (review), Mol. Membr. Biol. 15 (1998) 59–68, https://doi.org/10.3109/09687689809027519.

[36] H. Mi, D. Wang, Y. Xue, Z. Zhang, J. Niu, Y. Hong, K. Drlica, X. Zhao, Dimethyl sulfoxide protects *Escherichia coli* from rapid antimicrobial-mediated killing, Antimicrob. Agents Chemother. (2016), https://doi.org/10.1128/AAC.03003-15.

[37] M.E. Sweet, C. Larsen, X. Zhang, M. Schlame, B.P. Pedersen, D.L. Stokes, Structural basis for potassium transport in prokaryotes by KdpFABC, Proc. Natl. Acad. Sci. 118 (2021), https://doi.org/10.1073/pnas.2105195118.

[38] S. Halder, K.K. Yadav, R. Sarkar, S. Mukherjee, P. Saha, S. Haldar, S. Karmakar, T. Sen, Alteration of zeta potential and membrane permeability in bacteria: a study with cationic agents, Springerplus 4 (2015) 672, https://doi.org/10.1186/s40064-015-1476-7.

[39] H.P. Fernandes, C.L. Cesar, M. de L. Barjas-Castro, Electrical properties of the red blood cell membrane and immunohematological investigation, Rev. Bras. Hematol. Hemoter. (2011), https://doi.org/10.5581/1516-8484.20110080.

[40] A.P.V. Ferreyra Maillard, J.C. Espeche, P. Maturana, A.C. Cutro, A. Hollmann, Zeta potential beyond materials science: applications to bacterial systems and to the development of novel antimicrobials, Biochim. Biophys. Acta Biomembr. 1863 (2021) 183597, https://doi.org/10.1016/j.bbamem.2021.183597.

[41] R. Notman, M. Noro, B.O. Malley, J. Anwar, Molecular basis for dimethylsulfoxide (DMSO) action on lipid membranes, J. Am. Chem. Soc. 128 (2006) 13982–13983, https://doi.org/10.1021/ja063363t.

[42] M. Jen, K. Jeon, S. Lee, S. Hwang, W.J. Chung, Y. Pang, Ultrafast intramolecular proton transfer reactions and solvation dynamics of DMSO, Struct. Dyn. (2019), https://doi.org/10.1063/1.5129446.

[43] Y.C. Wen, H.C. Kuo, H.W. Jia, Multinuclear NMR spectroscopy for differentiation of molecular configurations and solvent properties between acetone and dimethyl sulfoxide, J. Mol. Struct. (2016), https://doi.org/10.1016/j.molstruc.2016.01.004.

[44] E. Kłodzińska, M. Szumski, E. Dziubakiewicz, K. Hrynkiewicz, E. Skwarek, W. Janusz, B. Buszewski, Effect of zeta potential value on bacterial behavior during electrophoretic separation, Electrophoresis 31 (2010) 1590–1596, https://doi.org/10.1002/elps.200900559.

[45] M. Szumski, E. Kłodzińska, E. Dziubakiewicz, K. Hrynkiewicz, B. Buszewski, Effect of applied voltage on viability of bacteria during separation under electrophoretic conditions, J. Liq. Chromatogr. Relat. Technol. 34 (2011) 2689–2698, https://doi.org/10.1080/10826076.2011.593223.

[46] H. Ranawat, N. Mazumder, T.S. Murali, K.K. Mahato, K. Satyamoorthy, Deciphering biophysical signatures for microbiological applications, Lasers Med. Sci. 35 (2020) 1493–1501, https://doi.org/10.1007/s10103-019-02936-9.

[47] A.J. Wyness, D.M. Paterson, E.C. Defew, M.I. Stutter, L.M. Avery, The role of zeta potential in the adhesion of *E. coli* to suspended intertidal sediments, Water Res. 142 (2018) 159–166, https://doi.org/10.1016/j.watres.2018.05.054.

[48] G. Dyrda, E. Boniewska-Bernacka, D. Man, K. Barchiewicz, R. Słota, The effect of organic solvents on selected microorganisms and model liposome membrane, Mol. Biol. Rep. (2019), https://doi.org/10.1007/s11033-019-04782-y.

[49] R. Notman, W.K. den Otter, M.G. Noro, W.J. Briels, J. Anwar, The permeability enhancing mechanism of DMSO in ceramide bilayers simulated by molecular dynamics, Biophys. J. 93 (2007) 2056–2068, https://doi.org/10.1529/biophysj.107.104703.

[50] R. Gurbanov, N.S. Ozek, S. Tunçer, F. Severcan, A.G. Gozen, Aspects of silver tolerance in bacteria: infrared spectral changes and epigenetic clues, J. Biophotonics 11 (2018), https://doi.org/10.1002/jbio.201700252.
[51] V. Dritsa, FT-IR spectroscopy in medicine, in: P.T. Theophile (Ed.), Infrared Spectrosc. - Life Biomed. Sci, InTech, 2012, https://doi.org/10.5772/37049.
[52] A. Dogan, K. Ergen, F. Budak, F. Severcan, Evaluation of disseminated candidiasis on an experimental animal model: a Fourier transform infrared study, Appl. Spectrosc. 61 (2007) 199–203, https://doi.org/10.1366/000370207779947459.
[53] B. Szalontai, Y. Nishiyama, Z. Gombos, N. Murata, Membrane dynamics as seen by Fourier transform infrared spectroscopy in a cyanobacterium, *Synechocystis* PCC 6803, Biochim. Biophys. Acta Biomembr. 1509 (2000) 409–419, https://doi.org/10.1016/S0005-2736(00)00323-0.
[54] V. Shapaval, N.K. Afseth, G. Vogt, A. Kohler, Fourier transform infrared spectroscopy for the prediction of fatty acid profiles in *Mucor* fungi grown in media with different carbon sources, Microb. Cell Factories 13 (2014) 86, https://doi.org/10.1186/1475-2859-13-86.
[55] M. Soleimani Aghdam, M. Asghari, M. Babalar, M.A. Askari Sarcheshmeh, Impact of salicylic acid on postharvest physiology of fruits and vegetables, in: Eco-Friendly Technol. Postharvest Prod, Qual, 2016, https://doi.org/10.1016/B978-0-12-804313-4.00008-6.
[56] L.B. Dreier, M. Bonn, E.H.G. Backus, Hydration and orientation of carbonyl groups in oppositely charged lipid monolayers on water, J. Phys. Chem. B (2019), https://doi.org/10.1021/acs.jpcb.8b12297.
[57] P.V. Dludla, B. Jack, A. Viraragavan, C. Pheiffer, R. Johnson, J. Louw, C.J. F. Muller, A dose-dependent effect of dimethyl sulfoxide on lipid content, cell viability and oxidative stress in 3T3-L1 adipocytes, Toxicol. Rep. (2018), https://doi.org/10.1016/j.toxrep.2018.10.002.
[58] S.S. Alam, D.L. Layman, Dimethyl sulfoxide as a cholesterol-lowering agent in cultured fibroblasts exposed to low density lipoproteins, Biochim. Biophys. Acta Lipids Lipid Metab. 710 (1982) 306–313, https://doi.org/10.1016/0005-2760(82)90113-8.
[59] B. Gironi, M. Paolantoni, A. Nicoziani, A. Morresi, P. Sassi, Impact of dimethyl sulfoxide and natural lipid heterogeneity on the structural properties of sphingomyelin membranes, Vib. Spectrosc. (2020), https://doi.org/10.1016/j.vibspec.2020.103101.
[60] P. Kumari, S. Kaur, S. Sharma, H.K. Kashyap, Impact of amphiphilic molecules on the structure and stability of homogeneous sphingomyelin bilayer: insights from atomistic simulations, J. Chem. Phys. 148 (2018), https://doi.org/10.1063/1.5021310.
[61] B. Gironi, R. Oliva, L. Petraccone, M. Paolantoni, A. Morresi, P. Del Vecchio, P. Sassi, Solvation properties of raft-like model membranes, Biochim. Biophys. Acta Biomembr. 1861 (2019) 183052, https://doi.org/10.1016/j.bbamem.2019.183052.
[62] A. Sadat, I.J. Joye, Peak fitting applied to Fourier transform infrared and Raman spectroscopic analysis of proteins, Appl. Sci. (2020), https://doi.org/10.3390/app10175918.
[63] S. Krimm, J. Bandekar, Vibrational spectroscopy and conformation of peptides, polypeptides, and proteins, Adv. Protein Chem. 38 (1986) 181–364, https://doi.org/10.1016/s0065-3233(08)60528-8.
[64] T. Takekiyo, Y. Yoshimura, A. Okuno, M. Kato, Pressure-induced amide I ' frequency shift of model compound of proteins in water, Proc. 4th Int, Conf. High Press. Biosci. Biotechnol. 1 (2007) 47–52. https://www.jstage.jst.go.jp/article/hpbb/1/1/1_1_47/_pdf.
[65] K.-Y. Chiang, F. Matsumura, C.-C. Yu, D. Qi, Y. Nagata, M. Bonn, K. Meister, True origin of amide I shifts observed in protein spectra obtained with sum frequency generation spectroscopy, J. Phys. Chem. Lett. 14 (2023) 4949–4954, https://doi.org/10.1021/acs.jpclett.3c00391.
[66] M.H. Ahmed, J.A. Byrne, J. McLaughlin, W. Ahmed, Study of human serum albumin adsorption and conformational change on DLC and silicon doped DLC using XPS and FTIR spectroscopy, J. Biomater. Nanobiotechnol. (2013), https://doi.org/10.4236/jbnb.2013.42024.
[67] J. Kong, S. Yu, Fourier transform infrared spectroscopic analysis of protein secondary structures, Acta Biochim. Biophys. Sin. Shanghai (2007), https://doi.org/10.1111/j.1745-7270.2007.00320.x.
[68] M. Di Foggia, M. Tsukada, P. Taddei, Vibrational study on the structure, bioactivity, and silver adsorption of silk fibroin fibers grafted with methacrylonitrile, Molecules (2023), https://doi.org/10.3390/molecules28062551.
[69] E. Dickinson, K.E. High, The use of infrared spectroscopy and chemometrics to investigate deterioration in vegetable tanned leather: potential applications in heritage science, Herit. Sci. (2022), https://doi.org/10.1186/s40494-022-00690-w.
[70] A. Tjernberg, N. Markova, W.J. Griffiths, D. HalléN, DMSO-related effects in protein characterization, J. Biomol. Screen. 11 (2006) 131–137, https://doi.org/10.1177/1087057105284218.
[71] Z.W. Yang, Dimethyl sulfoxide at 2.5% (v/v) alters the structural cooperativity and unfolding mechanism of dimeric bacterial NAD+ synthetase, Protein Sci. 13 (2004) 830–841, https://doi.org/10.1110/ps.03330104.
[72] D.S.H. Chan, D. Matak-Vinković, A.G. Coyne, C. Abell, Insight into protein conformation and subcharging by DMSO from native ion mobility mass spectrometry, ChemistrySelect (2016), https://doi.org/10.1002/slct.201601402.
[73] T. Arakawa, Y. Kita, S.N. Timasheff, Protein precipitation and denaturation by dimethyl sulfoxide, Biophys. Chem. 131 (2007) 62–70, https://doi.org/10.1016/j.bpc.2007.09.004.
[74] D.S.H. Chan, M.E. Kavanagh, K.J. McLean, A.W. Munro, D. Matak-Vinković, A. G. Coyne, C. Abell, Effect of DMSO on protein structure and interactions assessed by collision-induced dissociation and unfolding, Anal. Chem. 89 (2017) 9976–9983, https://doi.org/10.1021/acs.analchem.7b02329.
[75] J.H. Jeon, M. Javanainen, H. Martinez-Seara, R. Metzler, I. Vattulainen, Protein crowding in lipid bilayers gives rise to non-Gaussian anomalous lateral diffusion of phospholipids and proteins, Phys. Rev. X (2016), https://doi.org/10.1103/PhysRevX.6.021006.
[76] Y. Fang, B. Li, Y.L. Wang, L.B. Guo, G.C. Sun, FTIR analysis of *Burkholderia seminalis* from apricot, water and rice rhizosphere, Asian J. Chem. (2013), https://doi.org/10.14233/ajchem.2013.15212.
[77] E. Stępień, A. Kamińska, M. Surman, D. Karbowska, A. Wróbel, M. Przybyło, Fourier-transform infrared (FT-IR) spectroscopy to show alterations in molecular composition of EV subpopulations from melanoma cell lines in different malignancy, Biochem. Biophys. Rep. (2021), https://doi.org/10.1016/j.bbrep.2020.100888.
[78] E.K. Abdelwahed, N.A. Hussein, A. Moustafa, N.A. Moneib, R.K. Aziz, Gene networks and pathways involved in *Escherichia coli* response to multiple stressors, Microorganisms (2022), https://doi.org/10.3390/microorganisms10091793.
[79] M. Xu, T. Dai, Y. Wang, G. Yang, The incipient denaturation mechanism of DNA, RSC Adv. (2022), https://doi.org/10.1039/d2ra02480b.
[80] M. Iwatani, K. Ikegami, Y. Kremenska, N. Hattori, S. Tanaka, S. Yagi, K. Shiota, Dimethyl sulfoxide has an impact on epigenetic profile in mouse embryoid body, Stem Cells 24 (2006) 2549–2556, https://doi.org/10.1634/stemcells.2005-0427.
[81] R. Thaler, S. Spitzer, H. Karlic, K. Klaushofer, F. Varga, DMSO is a strong inducer of DNA hydroxymethylation in pre-osteoblastic MC3T3-E1 cells, Epigenetics 7 (2012) 635–651, https://doi.org/10.4161/epi.20163.
[82] E. Baldelli, M. Subramanian, A.M. Alsubaie, G. Oldaker, M. Emelianenko, E. El Gazzah, S. Baglivo, K.A. Hodge, F. Bianconi, V. Ludovini, L. Crino, E.F. Petricoin, M. Pierobon, Heterogeneous off-target effects of ultra-low dose dimethyl sulfoxide (DMSO) on targetable signaling events in lung cancer in vitro models, Int. J. Mol. Sci. 22 (2021) 2819, https://doi.org/10.3390/ijms22062819.